Available online at www.sciencedirect.com

ScienceDirect

Materials Today: Proceedings XX (2017) XXX–XXX

www.materialstoday.com/proceedings

ECT 2016

Heat Exchanger Performance Impacts on Optimum Cost Conditions in Thermoelectric Energy Recovery Designs

Terry J. Hendricks[a]*

Power and Sensors System Section
NASA-Jet Propulsion Laboratory, California Institute of Technology
4800 Oak Grove Drive, M.S. 277-207
Pasadena, CA 91109

Abstract

Cost is just as important as power density or efficiency for the adoption of waste heat recovery thermoelectric generators (TEG). Prior work [1] has shown that the system design that minimizes cost (e.g., the $/W value) can be close to the designs that maximize the system's efficiency or power density, however, it is important to understand the relationship between those designs to optimize TEG performance-cost compromises. Expanding on recent work [1, 2, 3] the impact of heat exchanger conditions on the optimum TEG fill factors and cost scaling of a waste heat recovery thermoelectric generator with a detailed treatment of the hot side exhaust heat exchanger has been investigated further. The effect of the heat lost to the environment and updated relationships between the hot-side and cold-side conductances [4] that maximize power output are considered. The optimum fill factor to minimize TEG energy recovery system costs is strongly dependent on the heat leakage fraction, σ, the mass flow rate of the exhaust, the hot-side heat exchanger effectiveness, heat exchanger UA_h, and heat flux. These relationships are explored and characterized for typical exhaust gas-flow conditions to show the inherent design complexities. The heat exchanger costs often dominate the TEG cost equation and it is critical to fully understand the tradeoff between heat exchanger performance, optimum TEG fill factors, and cost to establish potentially optimum design points within the cost-performance design space. This work will explore the design tradeoffs and relationships within the cost-efficiency-power density design space for a typical thermoelectric energy recovery system application. The interplay between optimum TEG fill factors and heat exchanger design can impact system footprint, volume, and mass in weight-sensitive applications. Less-effective, low-cost heat exchangers may outperform higher cost alternatives from a market adoption perspective. This shift of emphasis acknowledging the interdependence of optimum TEG fill factors and

* Corresponding author. Tel.: +1-818-354-4779.
E-mail address: terry.j.hendricks@jpl.nasa.gov

Selection and/or Peer-review under responsibility of the Conference Committee Members of 14th EUROPEAN CONFERENCE ON THERMOELECTRICS.

heat exchanger performance has significant implications on thermoelectric waste heat recovery systems designs and their operation. In addition, preferred TEG design regimes exist that accommodate reasonable compromises in TE performance and cost. This effort highlights how the optimum fill factor–heat exchanger performance relations couple to these optimum TEG performance-cost domains based on TEG-system-level analyses and provides a focus for future system research and development efforts.

Selection and/or Peer-review under responsibility of the Conference Committee Members of 14th EUROPEAN CONFERENCE ON THERMOELECTRICS.

Keywords: Thermoelectric systems; energy recovery; cost analysis; cost-performannce optimization; heat exchanger effects

1. Introduction

Thermoelectric (TE) energy recovery systems worldwide in industrial, automotive, military and spacecraft applications have a common need to demonstrate high performance; as measured by conversion efficiency, power output, power density, or heat or power flux, and low cost to be competitive with various energy conversion technologies. Recent focused attention has been given to cost modeling of cost per watt metrics associated with thermoelectric systems [1, 2, 3], in order to evaluate and quantify current cost levels and future potential cost levels for this technology in various energy recovery applications. Comprehensive TE / heat exchanger performance models have been extensively discussed in the literature [4-7]. However, detailed TE/heat exchanger performance – cost analysis models are not readily available or not generally reported on in energy recovery applications. Key system challenges and commercialization barriers are not so much TE performance anymore as they are system-level thermoelectric generator (TEG) costs in energy recovery (ER) applications, such that cost modeling and integrating cost modeling with system-level performance modeling is now critical. LeBlanc et al. [2] and Yee et al. [3] initially investigated cost modeling using simplified TE performance-cost models to get first order estimates of TE system level costs applicable to energy recovery systems. Hendricks et al. [1] followed this work with integration of detailed TE/heat exchanger performance models coupled with the cost modeling to better understand and quantity the cost metrics of real-world TE systems including detailed heat exchanger effects. This work seeks to expand those efforts in seeking a formalized, comprehensive approach that provides a more complete understanding of TE / heat exchanger integration coupled with cost modeling effects. This paper describes detailed thermal / TE system analysis models coupled with the cost modeling work of LeBlanc et al., Yee et al, and Hendricks et al. The effects of TE fill factor and heat exchanger mass flow rate, thermal effectiveness, and heat flux are examined to understand and quantify their impacts and interrelationships in coupled, integrated TE performance-cost modeling. The integrated thermal / TE / cost analysis models are then used to explore the various optimum specific power, efficiency, power, and cost regions and their relationships within the overall TEG system design domain for a given ER application.

Nomenclature

English

A_{HEX} – TE/Heat Exchanger Interface Area [m^2]
A_{TE} – Thermoelectric Element Area [m^2]
C_{TEG} – Thermoelectric Generator Cost [$]
C_{HEX} – Heat Exchanger Cost Parameter [$/(W/K)]
C'' - TE System Manufacturing/Fabrication Costs per Area [$/$m^2$]
C''' - TE Material Volumetric Costs per Volume [$/$m^3$]
C_p - Exhaust Flow Specific Heat [J/kg-K]
F - Fill Factor
F_{opt} – Optimum Cost Fill Factor
G – Thermoelectric System Cost per Watt [$/W]
K_H – Hot Side Total Thermal Conductance [W/K]

K_C – Cold Side Total Thermal Conductance [W/K]
K_{HX} – Heat Exchanger Conductance Value [W/K]
L – Thermoelectric Element Length [m]
$\dot{m}_h$ - exhaust mass flow rate [kg/sec]
N – Number of Thermoelectric Couples
I – Thermoelectric Device Current [A]
q – Thermal Flux [W/m^2]
Q – Thermal Transfer on Hot- or Cold-Side [W]
UA – Heat Exchanger UA Value [W/K]
V - Thermoelectric Device Voltage [V]
T – Temperature [K]

Greek
ε - Heat Exchanger Thermal Effectiveness
γ - Thermoelectric Element Length to Area Ratio [m^{-1}]
η - Thermoelectric Conversion Efficiency
σ - Heat Loss Factor Quantifying System Heat Losses ($=Q_{loss}/Q_{h,TE}$)

Subscripts
amb – ambient environment
exh – exhaust conditions
h – associated with TE hot-side parameter
c – associated with TE cold-side parameter
n – associated with TE n-type materials
p – associated with TE p-type materials
TE – Thermoelectric parameter
HEX – Heat Exchanger parameter

2. Thermal / Thermoelectric System Analysis Models

The thermal / TE system modeling starts with the thermoelectric system modeling work of Hendricks and Lustbader [5] and Hendricks and Crane [6] with additional modifications as detailed below. The TE fill factor is standardly defined as:

$$F = \frac{A_{TE}}{A_{HEX}} \tag{1}$$

at the interface between heat exchanger surfaces and thermoelectric device surfaces. As such, hot-side interfacial thermal energy balance requires that hot-side heat exchanger heat fluxes and hot-side thermoelectric heat fluxes are related through the fill factor:

$$q_{h,HEX} = F \cdot q_{h,TE} = \frac{Q_{h,TE} + Q_{loss}}{A_{HEX}} = f_Q(T_{exh}, T_h, T_c) \tag{2}$$

In using this relation, one must be very careful to not confuse interfacial heat fluxes with interfacial heat flows. In addition, the fill factor can also be interpreted as "funneling factor", whereby the hot-side thermoelectric heat flux is actually increased over the hot-side heat exchanger heat flux by the "thermal funneling" of heat flow from the heat exchanger into the thermoelectric device. The following equations 3-8 described the TE voltage - V, current - I, power (V*I), hot-side and cold-side thermal flows – Q_h and Q_c respectively, TE element geometry factors - γ_p and γ_n , and TE conversion efficiency relations inherent to this modeling approach. They define the fundamental relationships and linkage between voltage, current, power, thermal flows and conversion efficiency and the TE module geometry, TE

fill factor, and heat exchanger interface area, A_{HEX}.

$$\left(\frac{V}{N}\right)^{*} = f_v(T_h, T_c) \tag{3}$$

$$(I \cdot \frac{L}{F \cdot A_{HEX}})^{*} = f_I(T_h, T_c) \tag{4}$$

$$\left(\frac{Q_{h,TE} \cdot L}{N \cdot \mathrm{F} \cdot \mathrm{A}_{\mathrm{HEX}}}\right)^{*} = f_{qh}(T_h, T_c) \tag{5}$$

$$\left(\frac{Q_{c,TE} \cdot L}{N \cdot F \cdot A_{HEX}}\right)^{*} = f_{qc}(T_h, T_c) \tag{6}$$

$$\left(\frac{\gamma_p}{\gamma_n}\right)^{*} = f_A(T_h, T_c) \tag{7}$$

$$\eta_{TE}^{*} = \frac{P}{Q_{h,TE}} = f_{eff}(T_h, T_c) \tag{8}$$

Work by Hendricks et al. [1, 5] has also shown that hot-side thermal transfer is given by:

$$Q_{h,TE} = \frac{\left(T_{exh} - T_h\right) \cdot \left(1 - \sigma_{TE,h}\right)}{\left[\frac{1}{\dot{m}_h \cdot C_p \cdot \varepsilon_h \cdot \left(1 - \sigma_{HEX,h}\right)} + \frac{1}{K_{HX}}\right]} = K_h(T_{exh} - T_h) \tag{9}$$

and the cold-side thermal transfer is given by a similar expression:

$$Q_{c,TE} = K_c(T_c - T_{amb}) \tag{10}$$

where hot-side heat exchanger effectiveness is defined by:

$$\varepsilon_h = 1 - \exp(\frac{-UA_h}{\dot{m}_h \cdot C_p}) \tag{11}$$

These equations form a self-consistent set of equations that are functions of hot- and cold-side temperatures and exhaust temperature, as described in Hendricks and Crane [6], that define the complete coupled relationship between the heat exchanger design and the TE device design. The additional terms, TE fill factor, F, and heat exchanger interface area, A_{HEX}, are additional factors to solving these equations, which are tied to this set of performance equations through the additional information in Eq. 2. These equations point out and highlight that the TE fill factor and heat exchanger interfacial area are not "arbitrarily selected" parameters, but instead inherently tied to optimum TE design points at each point in the design space and any desired interfacial heat flux requirements. In most applications, the heat exchanger interface flux, $q_{h,HEX}$, usually has a "target" design value that the application is pursuing to satisfy system volume, weight and/or footprint area requirements. The goal is to use these relationships to determine optimum TE/heat exchanger designs within the overall system design space defined and bounded by the exhaust temperature, T_{exh}, TE hot-side temperature, T_h, TE cold-side temperature, T_c, and ambient temperature, T_{amb}. The complicating factors TE fill factor, interfacial heat fluxes, and the heat exchanger interface area are related by Eq. 2 and provide the ultimate foundation to cost analyses discussed below.

3. System Cost Analysis

The cost analysis leverages work by LeBlanc et al. [2] and Yee et al. [3], with enhancements as discussed in Hendricks et al. [1]. The total TE system cost is defined by [1, 2, 3]:

$$C_{TEG}[\$] = \left(C''' \cdot L_{TE} + C''\right) \cdot F \cdot A_{HEX} + \left(C_{HEX,h} \cdot K_H + C_{HEX,c} \cdot K_C\right) \tag{12}$$

where the three cost components are volumetric costs associated with TE materials, aerial-related fabrication costs, and heat exchanger costs. Hendricks et al. [1] leveraged the work of Yee et al. [3] and LeBlanc et al. [2] to show that the optimum fill factor to minimize the cost per watt metric is given by:

$$F_{opt} \approx \frac{1}{2} \cdot \sqrt{\frac{C_{HEX,h} + C_{HEX,c}}{C''' \cdot \kappa_{TE}}} \cdot \left(\frac{\dot{m} \cdot C_p \cdot \varepsilon_h \cdot \left(1 - \sigma_{HEX,h}\right) \cdot K_{HX}}{K_{HX} \cdot A_{tothex} + \dot{m} \cdot C_p \cdot \varepsilon_h \cdot \left(1 - \sigma_{HEX,h}\right) \cdot A_{tothex}} \right) \tag{13}$$

$$\lim_{K_{HX} >> \dot{m} \cdot C_p \cdot \varepsilon} F_{opt} \rightarrow \frac{1}{2} \cdot \sqrt{\frac{C_{HEX,h} + C_{HEX,c}}{C''' \cdot \kappa_{TE}}} \cdot \left(\frac{\dot{m}_h \cdot C_p \cdot \varepsilon_h}{A_{tothex}} \right) \cdot \left(1 - \sigma_{HEX,h}\right) \tag{14}$$

Yee et al. [3] first developed the form of this equation to establish the general functional relationship between F_{opt} and heat exchanger performance. Hendricks et al. [1] followed that work to establish the functional relationship between F_{opt} and key hot-side heat exchanger design parameters shown in Eqs. 13 and 14. Both of these relationships developed in Yee et al. [3] and Hendricks et al. [1] have their original heritage in the early-on work by Yee et al. [3] that establishes the general functional relationship. There were some fundamental inherent assumptions described by Yee et al. [3] that make this equation only approximate in the sense that it identifies the 0^{th}-order relationship with cost and heat exchanger parameters. The analysis by Yee et al. that led to the functional form of this equation assumed: 1) Thermal matching of hot-side and cold-side heat exchangers; 2) Not accounting for heat exchanger heat flux effects; 3) Equivalency of 3 key, very distinctly different heat exchanger areas, A_{TE} – TE device area, A_{HEX} – TE/Heat Exchanger Interfacial Area, and A_u – Heat Exchange Area Associated with UA; and 4) $K_H = UA_{HEX}$. Yee et al. [3] developed the general form of the equation for cost per watt, G, using these assumptions. A more rigorous modified equation for cost per watt, G, has been developed in this work by eliminating these assumptions and analysing a more realistic cost per watt relationship:

$$G = \frac{4 \cdot (m+1)^2}{{S_{pn}}^2 \cdot \sigma \cdot m \cdot \left(T_{exh} - T_{amb}\right)^2} \cdot \left[\frac{1.1 \cdot \kappa_{TE} \cdot A_{HEX} \cdot F}{K_H} + L_{TE} \right]^2 \cdot \left[C''' + \frac{C''}{L_{TE}} + \frac{C_{HEX} \cdot UA_u}{A_{HEX} \cdot L_{TE} \cdot F} \right] \tag{15}$$

which results when invoking the relationship $K_C \geq 10K_H$ from Hendricks [4]. When using this modified cost per watt, G, relationship and correcting these assumptions, the $\partial G/\partial F = 0$ condition yields a much more comprehensive and complex relationship for F_{opt}:

$$F_{opt} = \frac{-\left(\frac{\left(C_{HEX,h} + C_{HEX,c}\right) \cdot UA_u}{L_{TE}}\right) \cdot \left(\frac{1.1 \cdot \kappa_{TE}}{K_H}\right) + \sqrt{\left(\frac{\left(C_{HEX,h} + C_{HEX,c}\right) \cdot UA_u}{L_{TE}}\right)^2 \cdot \left(\frac{1.1 \cdot \kappa_{TE}}{K_H}\right)^2 + 8.8 \cdot \left(C''' + C''/L_{TE}\right) \cdot \left(\frac{\kappa_{TE}}{K_H}\right) \left(C_{HEX,h} + C_{HEX,c}\right) \cdot UA_u}}{4.4 \cdot \left(C''' + C''/L_{TE}\right) \cdot \left(\frac{\kappa_{TE} \cdot A_{HEX}}{K_H}\right)} \tag{16}$$

This is not in contradiction to the work by Yee et al. [3], which was critical to establishing the fundamental relationships, but merely a more thorough, comprehensive relationship that occurs when dispensing with all the simplifying assumptions pointed out above. It is clear that Eq. 16 in fact includes the fundamental dimensional groups initially determined by Yee et al. This new F_{opt} relationship also depends on the same cost parameters identified by Yee et al. [3] and Hendricks et al. [1] in Eq. 13. It provides a more accurate representation of the F-dependency on UA_u and interfacial heat flux, $q_{h,HEX}$, which will be shown below. The terms UA_h and UA_u will be used interchangeably in the following discussions since A_u and A_h are the same here.

4. Results and Discussion

4.1 Identifying High Specific Power Design Regions

This work focuses on a terrestrial energy recovery application that has an 823 K exhaust temperature (i.e., T_{exh}) and ambient temperatures (T_{amb}) < 273 K and the goal is to determine the optimum TE/heat exchanger design characteristics and ultimate cost metrics associated with this potential design. This particular design is targeting typical skutterudite materials and bismuth telluride materials fabricated and tested at NASA's Jet Propulsion Laboratory (JPL) in a segmented-element TE device design to achieve high efficiency and high specific power (W/kg). These materials are presented in Hendricks et al. [1] and Fleurial et al. [8]. Different performance metrics can be the design optimization objective; maximum efficiency, maximum power output, maximum power flux or maximum specific power. Many applications seek to maximize conversion efficiency or power output; however, in this particular terrestrial design case the design optimization objective is maximum specific power. This is somewhat different optimization objective and it is instructive and insightful to see how this aligns with the more conventional optimization objectives focused on maximum efficiency or maximum power. Figure 1a shows the TE device efficiency – power map with constant specific power lines superimposed showing how TE device specific power varies with efficiency and power in a TE power system operating under conditions associated with this application. Figure 1a shows the typical system design tradeoff between TE device efficiency and system power, while also showing TE device specific power increasing toward regions of higher efficiency in the system design space. These regions of high TE device specific power are exactly the starting point regions for high specific power TE system designs. It is insightful to know that regions of high TE device specific power (upper left corner) are actually not near the regions of maximum system power (lower right corner) in the TE device efficiency – power map, therefore one encounters a system design tradeoff. Later it will be shown that the highest power regions (lower device efficiency regions) also are associated with lowest cost per watt regions. This is the design challenge that thermoelectric power system technology continually faces and is perhaps not well known or internalized.

Equally important to understand in the context of Eq. 2 are the regions of required TE device heat flux in the efficiency – power map as shown in Figure 1b. One can see in Figure 1b that the regions of high TE device heat flux correspond to high specific power regions and high TE device efficiency. This represents a challenging TE device design region and further highlights the challenges of high specific power designs. One basically has to choose what TE system design region to work in: 1) high efficiency, high specific power regions, with corresponding high heat flux requirements, or 2) high power, low cost per watt regions.

Figure 2 shows the TEG cost per watt behavior as a function of power output that matches with the performance maps shown in Figure 1. This cost behavior is a direct result of Eqs. 12 and 15 relationships applied to this system design, with $C''' = 8.657 \times 10^4$ \$/m^3, $C'' = 168.2$ \$/m^2, and $C_{HEX,h}$ = \$1/(W/K) and $C_{HEX,c}$ = \$1/(W/K) in this analysis following the work of Hendricks et al. [1] and LeBlanc et al. [2]. It is demonstrated here that the low cost per watt regions are generally in the maximum power regions (occurring at the maximum power points in the analysis), but that cost per watt does asymptotically approach low values, which are not true minimums because of the asymptotic behavior. In Figure 2 is it also clear that heat exchanger costs are dominating the costs as evidenced by the 1/P behavior, similar to that found by Hendricks et al. [1].

Figure 3 shows the TEG cost per watt behavior as a function of TE device efficiency associated with the performance maps shown in Figure 1. The TEG cost per watt behavior here shows that the low cost regions are generally in the low efficiency regions of this design space, while TEG costs per watt increase at the higher TE device efficiencies. Hendricks et al. [1] discusses how there are not severe cost per watt penalties for operating in the TE preferred design regime, where efficiencies increase substantially from their minimums in this application, but TEG costs per watt only increase slightly from minimum values. Figure 3 also shows where high specific power regions are in relation to the TE preferred design regimes, and that these high specific power regions are generally at higher efficiencies than preferred design regimes because of their generally lower power levels.

Figures 1, 2 and 3 demonstrate the TE performance characteristics and design regions for this particular design application, similar to those discussed and presented by Hendricks et al. [1]. The new information associated with this application are: 1) the high specific power design regions and their relationship to and association with the high TE device efficiency regions (Figure 1a), and 2) the relationship to and association with the high specific power design regions and the high TE device heat flux regions in Figure 1b. This work highlights that these high specific power and minimum cost / high power design regimes do not coincide within the overall design domain in this application.

This is also a general conclusion for other design applications as the relative positions / locations of these design regimes are universal in all applications.

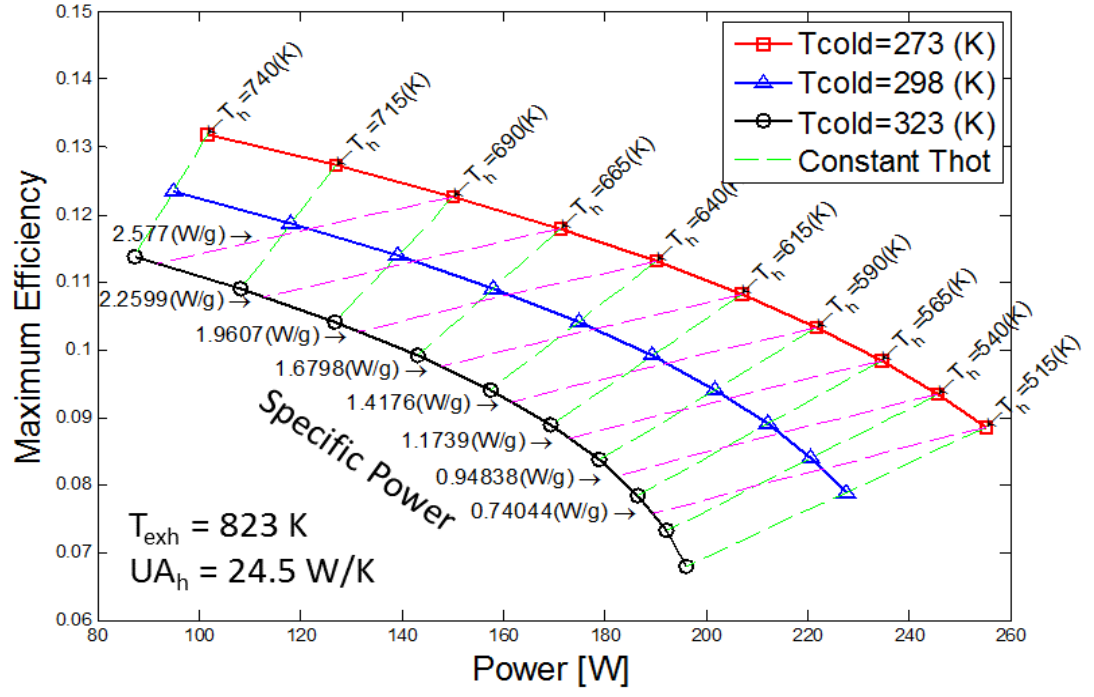

(a)

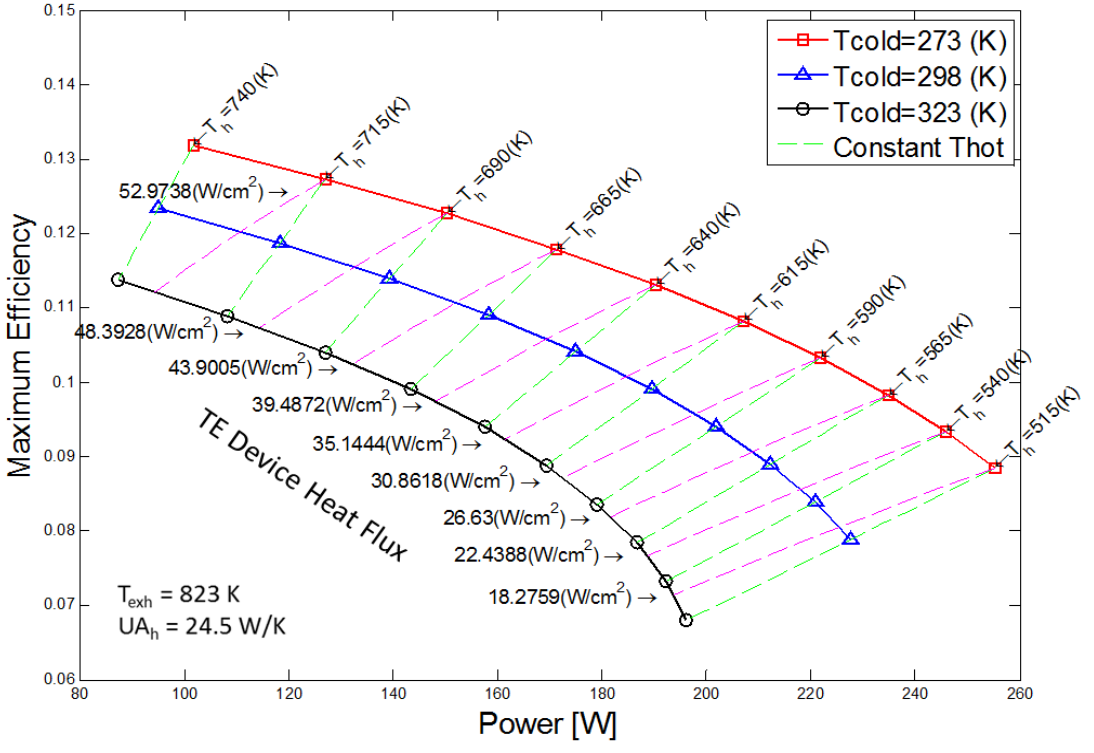

(b)

Figure 1 – Efficiency vs. Power with Constant Specific Power (a) and Constant Heat Flux Lines (b)

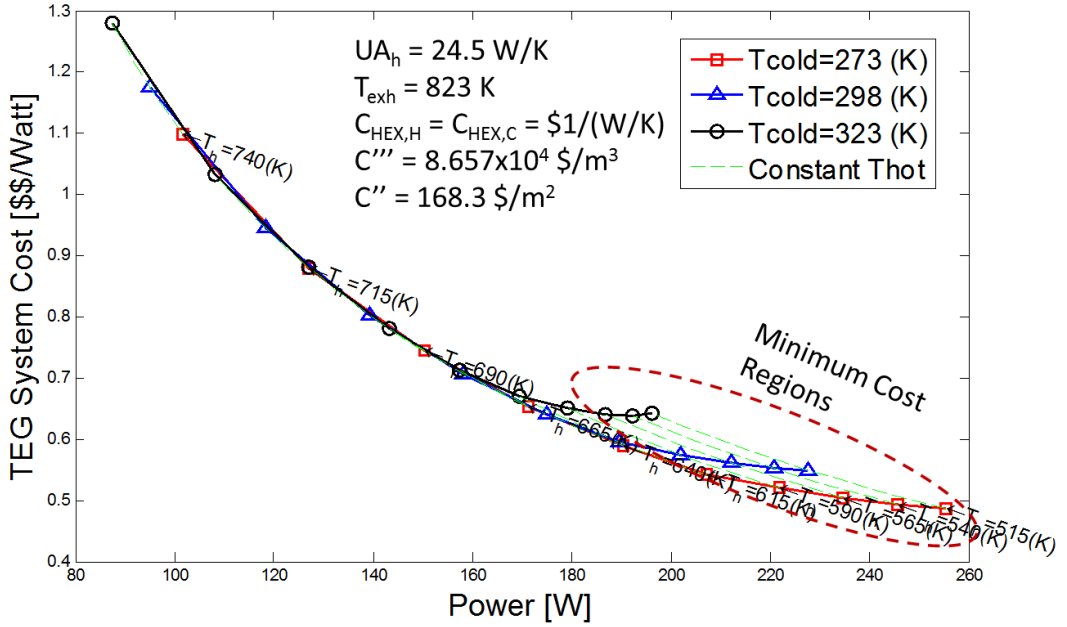

Figure 2 – Cost vs. Power in This Design Application with T_{exh} = 823 K and UA_h = 24.5 W/K and Given Cost Parameter, C''', C'', and C_{HEX} Parameters. Disclaimer: The cost information contained herein is of a budgetary and planning nature and intended for informational purposes only. It does not constitute a commitment on the part of Jet Propulsion Laboratory or California Institute of Technology.

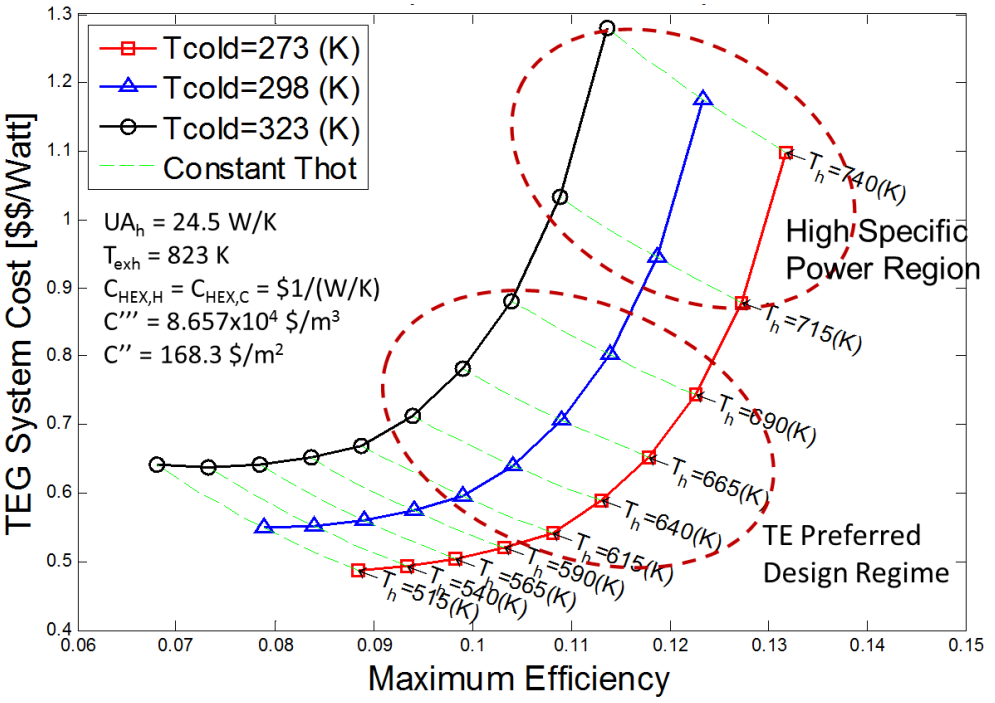

Figure 3 – Cost vs Efficiency in This Design Application with T_{exh} = 823 K and UA_h = 24.5 W/K and Given Cost Parameter, C''', C'', and C_{HEX} Parameters. Disclaimer: The cost information contained herein is of a budgetary and planning nature and intended for informational purposes only. It does not constitute a commitment on the part of Jet Propulsion Laboratory or California Institute of Technology.

The other new information is the fill factor, F, and heat exchanger area, A_{HEX}, that is simultaneously represented in and determined by solution of Eqs. 2-9. Eq. 2 in particular shows how the fill factor connects and associates the TE device heat flux to the heat exchanger interfacial heat flux. The TE device heat flux designs shown in Figure 1b and Eq. 2 can be used to determine various design fill factors throughout the design space in this application, but the fill factor does depend on the heat exchanger heat flux, which is often a design parameter given and established by the system design itself to satisfy system mass, volume, or areal footprint requirements. Figure 4 demonstrates the fill factor for three different heat exchanger heat fluxes, 5 W/cm^2, 10 W/cm^2, and 20 W/cm^2 at T_h = 705 K. It turns out that the fill factor relations can be determined for a targeted heat flux value at a specified T_h and a given design thermal conductance, K_H, at that condition (usually the case in any given design); then different heat flux conditions exist as one goes to various T_h cases on the curve because the heat flux for a given K_H is then dependent on the (T_{exh} – T_h condition at that point. The resulting F-relationship is that shown in Figure 4. These three fill factor charts are intimately coupled to the TE design points in TE device efficiency – power maps in Figure 1. Another approach could be to simply set a constant heat flux condition all along the curves in Figure 4 coupled to the TE design domain points in Figure 1. This would amount to having a different K_H condition along the F-curves. This could be done in certain preliminary design scoping studies when trying to identify preliminary TE design conditions, preferred design regimes, and possible heat flux conditions. The first approach (as shown in Figure 4) then provides a more realistic F-relationship when in more advanced, mature design stages.

Examining Figure 4 in conjunction with Figure 1 design points/regions demonstrates several major design themes: 1) Lower heat exchanger heat flux levels lead to lower fill factor requirements, 2) Higher fill factors are generally associated with the high power regions and lower costs per watt regions in Figures 1 and 2, 3) Lower fill factors are generally associated higher specific power regions, higher TE device heat flux regions, and higher TE device efficiency regions, and 4) Fill factor equal 1 shows that at certain high heat exchanger heat flux levels one can actually "saturate" the available heat exchanger area, which represents an unachievable condition where all available heat exchanger interface area is overly-filled with TE devices. The F=1 condition is achieved faster and more often when higher heat fluxes are targeted, so these F-curves quickly identify non-viable heat flux design conditions while mapping out the efficiency – power relations in Figure 1. It is also clear that the correct fill factor for optimum performance in a given application is not an "arbitrarily selected" design parameter – it is dependent on TE device and heat exchanger heat fluxes and the TE system design point selected in Figure 1.

4.1 Quasi-Optimum Fill Factor Relationships With TE / Heat Exchanger Parameters

It is useful, now that one knows of the existence of the F-relationships shown in Figure 4, to predict the optimum cost fill factor, F_{opt}, (i.e., or region) a priori, dependency of optimum cost fill factor on heat exchanger parameters, and how those a priori predictions align with the findings in Figure 4. One deficiency of Eq. 13 and the related equation in Yee et al. [3] is that it does not clearly show the dependency of F_{opt} on TE / heat exchanger interfacial heat flux, $q_{h,HEX}$ (See Eq. 2). Generally, one expects that the optimum fill factor will increase with both heat exchanger UA_u and with TE/heat exchanger interfacial heat flux, $q_{h,HEX}$. Eq. 16 provides the relation to explore this. The dependency on heat exchanger UA_u is clearly shown in Eq. 16, but the dependency on TE/heat exchanger interfacial heat flux is buried within the K_H or (K_H/A_{HEX}) terms in Eq. 16. This interfacial heat flux dependency in Eq. 16 becomes clearer when one realizes that this heat flux is related by:

$$q_{h,HEX} = \frac{K_H \cdot (T_{exh} - T_h)}{A_{HEX}} \qquad [17]$$

Once one makes the appropriate substitutions within Eq. 16 it is possible to highlight the $q_{h,HEX}$ effect on F_{opt}. The UA_h and $q_{h,HEX}$ effects on F_{opt} determined by analyzing a number of heat exchanger designs with varying UA_h and $q_{h,HEX}$ as part of the specific power optimization work discussed above. Figures 5 and 6 demonstrate the optimum cost fill factor relationship using Eq. 16 defined during the course of exploring and analysing these different heat exchanger designs in this application. Figure 5 shows the typical optimum cost fill factor dependency on hot-side heat exchanger UA_h (UA_u) performance using Eq. 16 for a constant L_{TE} and the typical design parameters in this

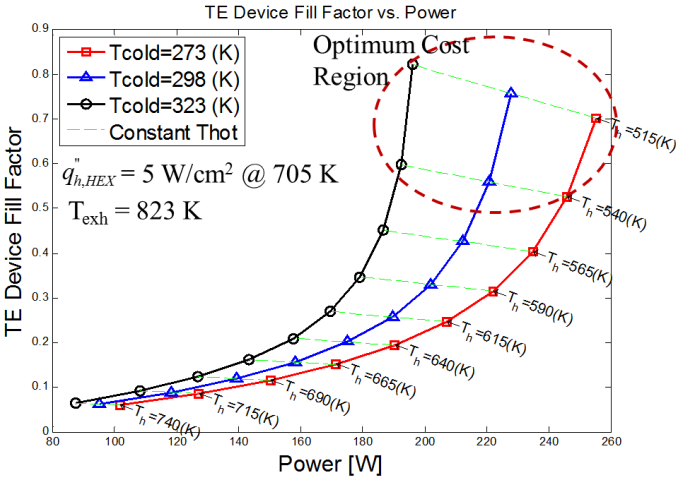

(a)

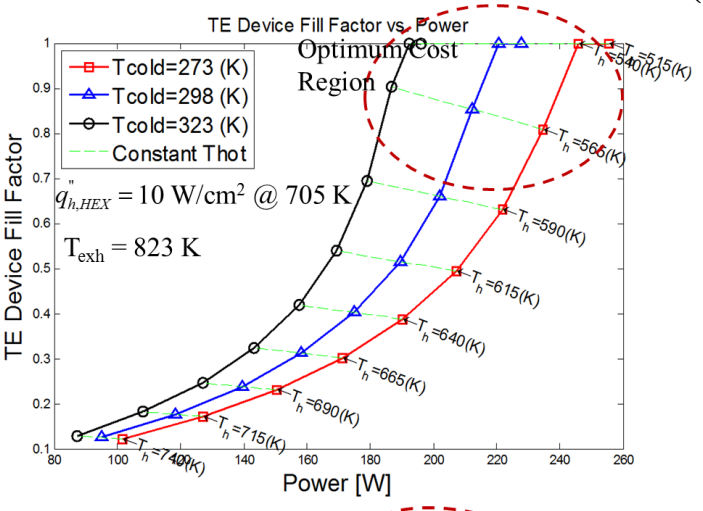

(b)

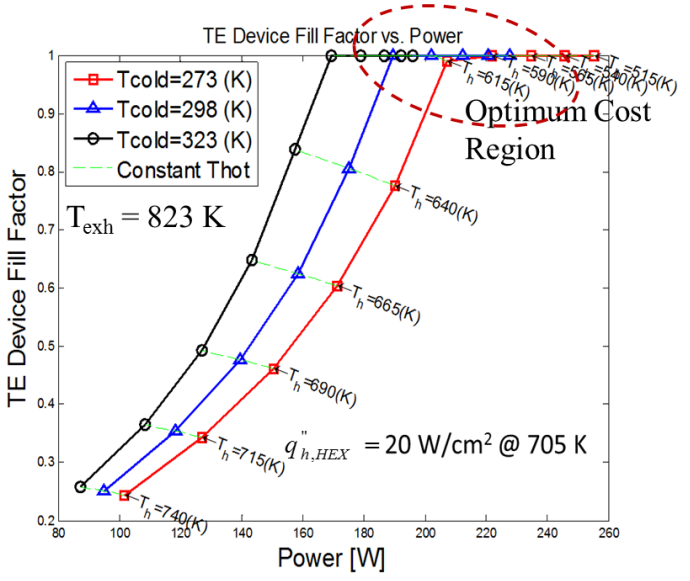

(c)

Figure 4 – Fill Factors for $q_{h,HEX}$ = 5 W/cm² at 705 K (a), 10 W/cm² at 705 K (b), and 20 W/cm² at 705 K (c) Respectively.

Table 1 – Current TEG Design Parameters Used in Eq. 16 for this Design & Cost Investigation

C''' [\$/m^3]	C'' [\$/m^2]	L_{TE} [mm]	κ_{TE} [W/m-K]	$C_{HEX,h}$, $C_{HEX,c}$ [\$/(W/K)]	$(T_{exh} - T_h)$ [K]
8.657x10^4	168.2	2.0	2.5	1.0	119

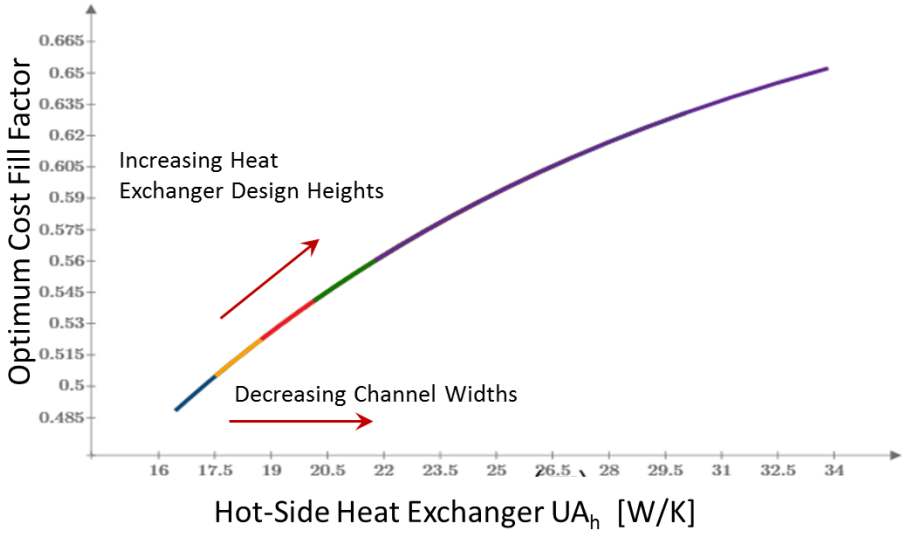

Figure$_u$ 5 – Optimum Cost Fill Factor Dependency on Heat Exchanger Parameters

application shown in Table 1. Eq. 16 defines the optimum cost fill factors for all the potential heat exchanger designs in this application according to the Figure 5 relationship. The different colored curves represent different heat exchanger designs having increasing heat exchanger design heights perpendicular to the given exhaust flow direction in this application. Increasing design heights are shown to generally increase the hot-side heat exchanger UA_h. The trend of decreasing channel widths is also shown with its impact of increasing the heat exchanger UA_h because this generally increases heat transfer coefficients and the heat transfer area within the heat exchanger. This clearly shows the general trends of heat exchanger design characteristics (design heights and channel widths) in the increasing UA_h direction and their impact on F_{opt} as they increase UA_h, thereby coupling these impacts to specific heat exchanger design parameters. The optimum fill factor generally increases non-linearly as the hot-side heat exchanger, UA_h, increases, indicating that the TEG design generally needs higher optimum cost fill factors as heat exchanger performance increases and drives more thermal energy into the TE devices. This modifies the finding of Yee et al. [1] and Hendricks et al. [3] which showed a linear dependency on UA_h (UA_u).

Figure 6 demonstrates the optimum cost fill factor relationship with interfacial heat flux at the TE device / heat exchanger interface using Eq. 16. Figure 6 is highly relevant in showing that the optimum cost fill factor, F_{opt}, is linearly dependent on the interfacial heat flux, $q_{h,HEX}$ and increases with $q_{h,HEX}$ as one should expect. This provides much more information than Eq. 13 and is a key finding of this work. Figure 6 also demonstrates, like Figure 5, the relevant trends and directions of increasing heat exchanger design height and decreasing channel widths in increasing interfacial heat flux, thereby coupling the directions of increasing/decreasing interfacial heat flux to specific heat exchanger design parameters. What is highly interesting in Figure 6a is the 11 W/cm^2 line indicates that F_{opt} = 0.65, which is approximately the optimum cost fill factor in the low cost region of Figure 4a where the interfacial heat flux is also about 11 W/cm^2. Figure 6b is equally interesting in that the 15 W/cm^2 line indicates F_{opt} = 0.86 (a rather high value indeed) and higher heat fluxes >16.25 W/cm^2 in Figure 6b show F_{opt} ~ 0.94 and approaching 1. This is approximately the optimum cost fill factor in the low cost region of Figure 4b where the interfacial heat flux is also approximately these levels. Eq. 16 therefore is doing reasonably good at a priori predicting where the optimum cost fill factor should reside in a full TEG system analysis in Figures 1-4. This is first time that a F_{opt} relationship has

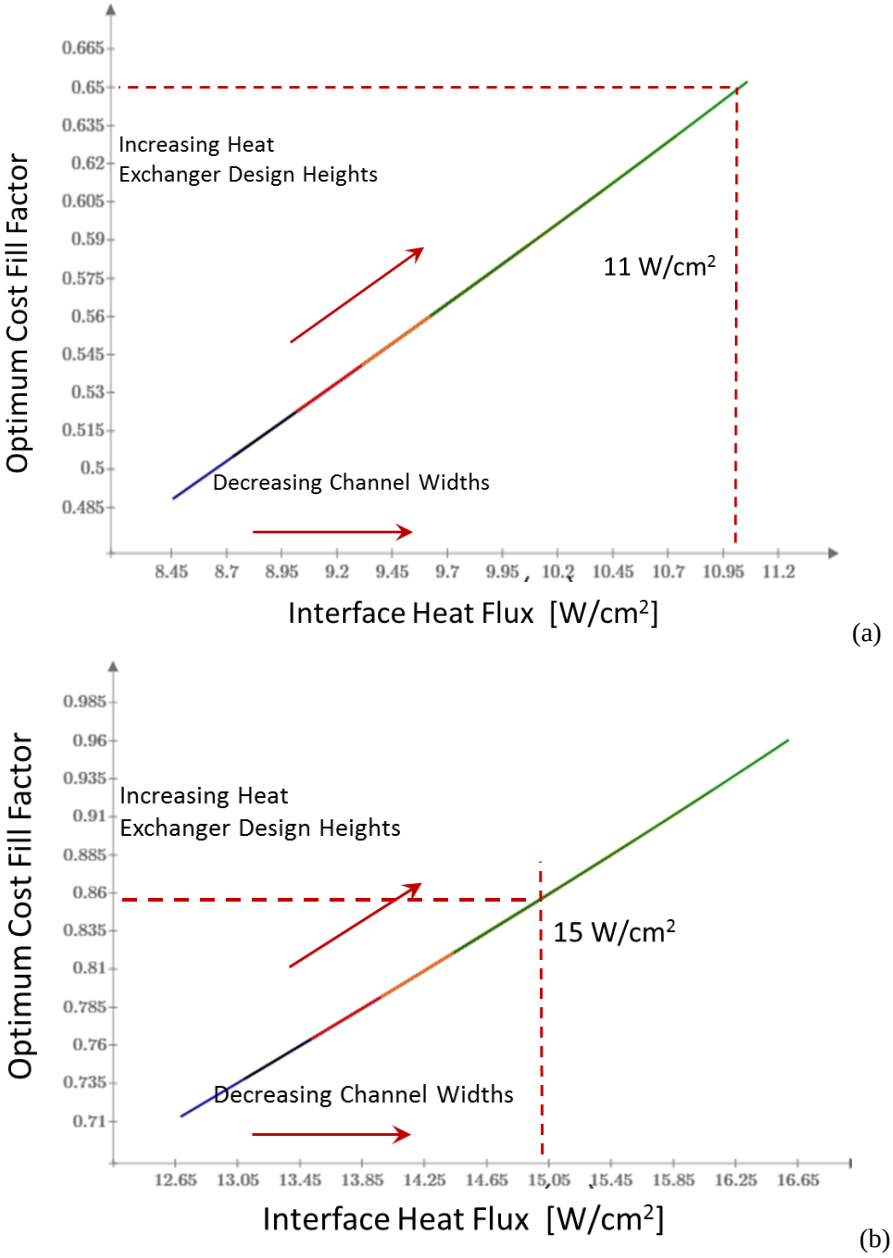

Figure 6 – Optimum Cost Fill Factor Dependency on Heat Exchanger Interface Heat Flux for Two Heat Flux Ranges

shown this capability to predict where the optimum cost fill factor should occur and how it is dependent on heat exchanger UA_h (UA_u), $q_{h,HEX}$, and the specific heat exchanger design parameters in the hot-side heat exchanger design. This is highly relevant to many waste heat recovery TEG designs in industrial, automotive and military applications and will help designers and program managers identify the low cost per watt regions and what TEG and heat exchanger characteristics and design parameters will allow one to achieve those regions.

4. Conclusions

Energy recovery designs that identify and seek to maximize high specific power designs are investigated and characterized. The mathematical framework and foundation is presented that allows one to simultaneously identify high specific power regions within the TEG performance (i.e., power and efficiency) optimization process. TE device fill factor, F, and the TE device/heat exchanger interfacial area, A_{HEX}, are now determined as part of the design optimization process and are no longer arbitrarily selected design parameters. This allow one to investigate the specific power characteristics of multiple designs throughout the overall TEG design domain. Locations of high specific power design regions in the overall TEG design domain are highlighted and discussed for a high-temperature energy recovery application where T_{exh}= 823K and T_{amb} < 273 K. This work has demonstrated the relationship of high specific power regions to high Efficiency, high power, and low cost per watt design regions in the overall TEG system design domain. High specific power regions are characterized by high TE device heat flux, high TE device efficiency, and high cost per watt and associated with these design regions. The high TE device heat flux generally required by high specific power designs creates significant design challenges at the TE device level and the TE device / heat exchanger interfaces. These high specific power regimes are generally mutually exclusive with low cost per watt and high power regions, thereby creating significant TEG system design tradeoffs.

Cost analysis work has developed the mathematical foundation to identify low cost per watt regions simultaneously within the aforementioned TEG performance optimization process, thereby providing a key computational cost-performance design optimization tool for simultaneously determining low cost per watt design regions and their relationship to high specific power, high efficiency and high power design regions. Low cost per watt regions are generally associated with high power regions and lower efficiency regions in the overall design domain. The TE device fill factor, F, and TE device/heat exchanger interfacial area, A_{HEX}, become integral design parameters within the TEG cost-performance optimization process and both design parameters impact the cost analysis within the performance optimization process. This work defines the resulting fill factor relationships determined as part of the design optimization process and shows the fill factor dependency on hot-side heat exchanger UA_h (UA_u) and the heat exchanger interfacial heat flux. A new, more comprehensive optimum cost fill factor (i.e., F_{opt}) relationship is presented, which can: 1) a priori establish optimum cost fill factors, F_{opt} , associated with low cost per watt design points in the TEG waste heat recovery design domain, and 2) more accurately accounts for heat exchanger UA_h (UA_u) and interfacial heat flux, $q_{h,HEX}$, effects on F_{opt}. F_{opt} dependency on hot-side heat exchanger UA_h and interfacial heat flux, $q_{h,HEX}$ are demonstrated which align better with known design characteristics in TEG waste heat recovery. F_{opt} increases non-linearly with hot-side heat exchanger UA_h and linearly with interfacial heat flux, $q_{h,HEX}$. This is highly relevant to many waste heat recovery TEG designs in industrial, automotive and military applications. This updated cost-performance optimization tool, its inherent mathematical foundation, and F_{opt} relationship enlightens designers and program managers on what TE device / heat exchanger characteristics and design parameters allow one to achieve low cost per watt regions. It more importantly quantifies the inherent system design tradeoffs and sensitivities in distinguishing high power, high efficiency, high specific power, and low cost per watt designs within the overall TEG design domain in high-temperature energy recovery applications.

Acknowledgements

This work was carried out under NASA Prime contract NNN12AA01C under JPL Task Plan No. 81-19765 with Defense Advanced Research Program Agency, at the Jet Propulsion Laboratory, California Institute of Technology, under a contract to the National Aeronautics and Space Administration. The author acknowledges Dr. Shannon Yee, George W. Woodruff School of Mechanical Engineering, Georgia Institute of Technology, Atlanta, GA and Dr. Saniya LeBlanc, School of Engineering and Applied Sciences, Department of Mechanical & Aerospace Engineering, George Washington University, Washington, DC for their many enlightening thoughts and conversations in this critical technical area.

References

[1] Hendricks, T. J., Yee, S. K., and LeBlanc, S., *Journal of Electronic Materials,* 2015, **45**, No. 3, 1751-1761, The Minerals, Metals, and Materials Society, Springer, DOI: 10.1007/s11664-015-4201-y.

[2] LeBlanc, S., Yee, S. K., Scullin, M. L., Dames, C., and Goodson, K. E., *Renewable and Sustainable Energy Reviews, 2014*, **32**, 313-327.

[3] Yee, S. K., LeBlanc, S., Goodson, K. E., and Dames, C. *Energy & Environmental Science*, 2013, **6**, 2561-2571.

[4] Hendricks, T.J., "Integrated Thermoelectric–Thermal System Resistance Optimization to Maximize Power Output in Thermoelectric Energy Recovery Systems, Mater. Res. Soc. Symp. Proceedings, 2014, **1642**, Materials Research Society, mrsf13-1642-bb02-04 doi:10.1557/opl.2014.443.

[5] Hendricks, T.J. and Lustbader, J. in *Proceedings of the 21st International Conference on Thermoelectrics (Long Beach, CA)*, 2002, IEEE Catalogue #02TH8657, p. 381.

[6] Hendricks, T.J. and Crane, D. "Thermoelectric Energy Recovery Systems: Thermal, Thermoelectric and Structural Considerations", **CRC Press Handbook of Thermoelectrics & Its Energy Harvesting: Modules, Systems, and Applications in Energy Harvesting**, Book 2, Section 3, Chapter 22, Taylor and Francis Group, Boca Raton, FL, 2012.

[7] Crane, DT and LE Bell, 2009, "Design to Maximize Performance of a Thermoelectric Power Generator With a Dynamic Thermal Power Source," *Journal of Energy Resources Technology*, 131:012401-1 to 8.

[8] J.-P. Fleurial, S.K. Bux, B.C.-Y. Li, S. Firdosy, N.R. Keyawa, P.K. Gogna, D.J. King, J.M. Ma, K. Star, A. Zevalkink, and T. Caillat, in Symposium BB: thermoelectric materials–from basic science to applications, Proceedings of 2013 Materials Research Society Fall Meeting, Boston (2013).